Coupled electron and hole quantum wires

J. S. Thakur
School of Physics, The University of New South Wales, Sydney 2052, Australia

D. Neilson
School of Physics, The University of New South Wales, Sydney 2052, Australia
and Scuola Normale Superiore, Piazza dei Cavalieri 7, 56126 Pisa, Italy
(Received 5 November 1996)

We have investigated the effect of many-body correlations on properties of coupled electron-hole quantum wires using a Singwi-Tosi-Land-Sjölander approach. At $r_s=4$ the acoustic collective mode traverses the single-electron excitation region as a narrow resonance peak and reemerges in the undamped region on the high-q side of the excitation region. The acoustic collective mode, but not the optic mode, is sensitive to the separation between the wires. For $r_s>2.5$ the effective interaction acting between the electrons which is mediated by the heavier holes becomes attractive when the separation between the wires drops to a critical value. For $0.8\leqslant r_s\leqslant 2.5$ we detect a charge-density-wave ground state for small wire separations. [S0163-1829(97)04931-X]

I. INTRODUCTION

The effect of interactions between electrons in parallel quantum wires embedded in a semiconductor substrate has been the subject of a number of recent investigations.[1–3] The strength of correlations within each wire increases as the electron density is decreased and the correlations between electrons in different wires also increases if the wires are brought closer together. Correlations can affect the properties of the collective modes of the coupled system and it may also lead to charge-density-wave instabilities.[1]

In this paper we look at the effect of correlations for two parallel quantum wires, one wire with electrons and the other with holes. This system differs in important ways from two coupled wires of electrons, not only because of the attractive interaction between the electrons and holes, but also because the effective masses of the electrons and holes are in general different and this makes the system asymmetric. Tunneling of carriers between parallel wires has been observed,[4] but we restrict ourselves here to cases where the tunneling amplitude is negligible. This can be because the wires are sufficiently far apart or because there is a repulsive potential barrier between the wires. We will use parameters appropriate for quantum wires embedded in a gallium arsenide substrate. Li and Das Sarma[5] and Gold and Ghazali[6] have investigated quantum wires in gallium arsenide theoretically.

The importance of correlations for coupled quantum wires is especially interesting when we recall that the ground state for electrons in an isolated and defect-free wire with a single subband is believed to be a Luttinger liquid. For a Luttinger liquid the excitation spectrum is saturated by the collective modes of the system so there are no single-particle excitations. However, the existence of defects[7] or the presence of a second wire both help to restore Fermi-liquid-like behavior, and it is interesting to map out the nature of the low-lying excitation spectrum. Of particular interest are the relative spectral strengths of the collective modes and the single-particle excitations.

We determine the properties of the ground state and low-lying excitations in zero magnetic field using the density-density response function matrix for two coupled wires. We calculate the matrix using a Singwi-Tosi-Land-Sjölander (STLS) zero-temperature approach[8] for a two-component system.[9] In STLS the static correlations are taken into account by replacing the Coulomb interactions with effective interactions between the particles. For a single wire Friesen and Bergersen,[10] Borges, Degani, and Hipolito,[11] and Campos, Degani, and Hipolito[12] have used STLS to calculate pair correlation functions and the properties of the plasmon collective mode. Thakur and Neilson used STLS to investigate the interdependence of the electron correlations and electron-defect scattering.[13]

The diagonalized response function matrix gives the pair correlation functions both for carriers within the same wire and for carriers in opposite wires. Singularities in the diagonalized matrix elements determine the dispersion curves of the collective modes and their spectral strengths. If any singularity is found in the static response function this is evidence for an instability in the liquid ground state to, for example, a charge-density-wave ground state.[14]

II. THEORY

We consider two parallel wires of the same finite diameter a separated by distance d. The effective masses of the electrons and holes are $m_e^\star$ and $m_h^\star$, respectively. We take the carrier density n in each wire equal. The bare Coulomb interactions between carriers in the same wire are $V_{ee}(q)=V_{hh}(q)=K_0(qa)$, where $K_0(q)$ is the zeroth-order modified Bessel function of the second kind. The bare Coulomb interactions between the electrons and holes are $V_{eh}(q)=V_{he}(q)=K_0(q\sqrt{a^2+d^2})$.

The density-density response function matrix elements within each wire $\chi_{ee}(q,\omega)$ and $\chi_{hh}(q,\omega)$, and the matrix elements between wires $\chi_{eh}(q,\omega)=\chi_{he}(q,\omega)$ are expressed in terms of the Lindhard function for noninteracting carriers

in a one-dimensional wire $\chi_i^{(0)}(q,\omega)$ (Ref. 15) and effective interactions between the carriers $\tilde{V}_{ij}(q)$ and $\tilde{\mathcal{V}}_{ij}(q)$,[9]

$$\chi_{ii}(q,\omega)=\frac{\chi_i^{(0)}(q,\omega)}{1-\tilde{\mathcal{V}}_{ii}(q,\omega)\chi_i^{(0)}(q,\omega)}, \quad i=e,h,$$
$$\chi_{eh}(q,\omega)=\frac{\chi_e(q,\omega)\tilde{V}_{eh}(q)\chi_h(q,\omega)}{1-\tilde{V}_{eh}^2(q)\chi_e(q,\omega)\chi_h(q,\omega)}, \tag{1}$$

where

$$\chi_i(q,\omega)=\frac{\chi_i^{(0)}(q,\omega)}{1-\tilde{V}_{ii}(q)\chi_i^{(0)}(q,\omega)}, \quad i=e,h. \tag{2}$$

The effective interactions in Eqs. (1) and (2),

$$\tilde{V}_{ij}(q)=V_{ij}(q)[1-G_{ij}(q)], \quad i,j=e,h,$$
$$\tilde{\mathcal{V}}_{ii}(q,\omega)=\tilde{V}_{ii}(q)+\tilde{V}_{ij}(q)\chi_j(q,\omega)\tilde{V}_{ji}(q), \quad i=e,h; \ j\neq i, \tag{3}$$

take into account the correlations between the carriers through local field factors $G_{ij}(q)$. We calculate the $G_{ij}(q)$ using the self-consistent method developed by Singwi *et al.*[8] In the STLS the local field $G_{ij}(q)$ is defined by the closure ansatz

$$G_{ij}(q)=-\frac{1}{n}\int\frac{dk}{(2\pi)}\frac{(qk)}{q^2}\frac{V_{ij}(k)}{V_{ij}(q)}[S_{ij}(|q-k|)-\delta_{ij}], \tag{4}$$

where the $S_{ij}(q)$ are the structure factors. The fluctuation-dissipation theorem relates $S_{ij}(q)$ to $\chi_{ij}(q,\omega)$,

$$S_{ij}(q)=\frac{1}{n}\int_0^\infty d\omega \ \chi_{ij}(q,i\omega). \tag{5}$$

Equations (1)–(5) are solved self-consistently. When diagonalized the response function matrix has elements

$$\chi_\pm(q,\omega)=\frac{1}{2}[\chi_{ee}(q,\omega)+\chi_{hh}(q,\omega) \pm\sqrt{[\chi_{ee}(q,\omega)-\chi_{hh}(q,\omega)]^2+4\chi_{eh}^2(q,\omega)}]. \tag{6}$$

III. RESULTS

A. Static properties

We use values for the dielectric $\epsilon=13$ and effective masses ratio $m_h^\star/m_e^\star=7$, appropriate for wires embedded in a gallium arsenide substrate. The wire diameter is fixed at $a/a_0^\star=4/\pi$ where the effective Bohr radius for electrons is $a_0^\star=\hbar^2\epsilon/m_e^\star e^2=9.8$ nm. For holes the effective Bohr radius is 1.4 nm, which makes r_s^h in the hole wire seven times larger than r_s^e in the electron wire for equal carrier densities.

In Fig. 1 we plot the pair correlation functions $g_{ij}(r)$ as a

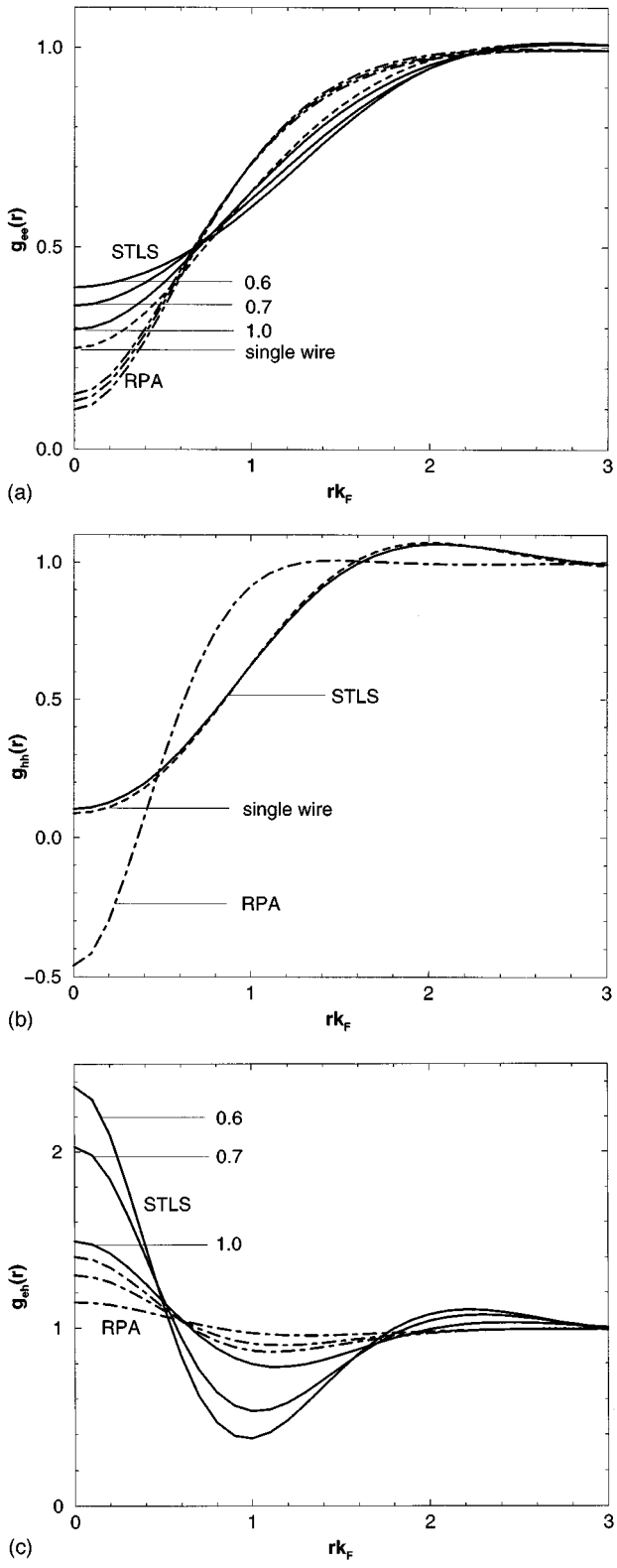

FIG. 1. (a) Pair correlation function $g_{ee}(r)$ for electron wire. The electron density parameter is $r_s^e=2$. Labels denote wire separation dk_F. Solid lines: present calculation. Dash-dotted lines: RPA for same range of d. Dashed lines: STLS calculation for single wire. (b) $g_{hh}(r)$ for the same parameters as in (a). Curves for the different d are not distinguishable on this scale. (c) $g_{eh}(r)$ for the same parameters and labels as (a).

function of the separation between the wires. The value of the density parameter for the electrons is $r_s^e=2$ (and hence $r_s^h=14$ for the holes). Also shown are the corresponding RPA results. In the RPA the local fields are zero and there are no correlations.

Figure 1(a) shows the pair correlation functions in the electron wire. $g_{ee}(r)$ decreases with r as two electrons approach each other. This is the well-known exchange-correlation hole caused by the repulsion between electrons. As the wires are brought closer together the correlations between electrons and holes build up the density of holes opposite to any point where there are two electrons near each other. This buildup of holes partially cancels the repulsion between the electrons and partially fills in the exchange-correlation hole. The effect is strongest when the two electrons are very close together. Comparing this with the $g_{ee}(r)$ for a single isolated electron wire demonstrates the importance of electron-hole interactions on $g_{ee}(r)$. In the random-phase approximation (RPA) there is no strong buildup of hole density opposite an electron and $g_{ee}(r)$ is not affected by the proximity of the hole wire.

Figure 1(b) shows the pair correlation function in the hole wire. The structure of $g_{hh}(r)$ is determined primarily by the direct correlations between the holes because r_s^h is so large. $g_{hh}(r)$ is similar to the $g_{hh}(r)$ for an isolated hole wire at the same r_s^h, so $g_{hh}(r)$ is not greatly affected by the adjacent electron wire. The RPA $g_{hh}(r)$ is also insensitive to the presence of the electron wire. In the RPA $g_{hh}(r)$ for small r is unphysical because it is negative. A breakdown of the RPA usually indicates the existence of strong correlations.

The correlation function between the wires $g_{eh}(r)$ is shown in Fig. 1(c). As the wires are brought closer together $g_{eh}(r)$ for small r increases rapidly. This indicates a strong buildup of hole density opposite each electron and vice versa. The oscillations in $g_{eh}(r)$ at larger r become more pronounced as the wire separation d is decreased. In the RPA $g_{eh}(r)$ does not show these strong effects, indicating that without correlations the two wires are relatively weakly coupled.

Figure 2 shows the dependence of the correlation functions on the carrier densities for fixed wire separation. As the density is decreased the correlations become stronger and the differences between the $g_{ij}(r)$ in the present calculation and the RPA $g_{ij}(r)$ become larger. Because $r_s^h \gg r_s^e$ the correlations in the hole wire are stronger than those in the electron wire. For the lowest density shown, $r_s^e=4$, the $g_{eh}(r)$ develops a large peak at small r. This peak may reflect a tendency toward the formation of excitons.[16] There is a concurrent dip in $g_{eh}(r)$ centered about $rk_F \simeq 1$, where k_F is the Fermi momentum. At $r_s^e=4$ not only the RPA $g_{hh}(r)$ but also the RPA $g_{ee}(r)$ goes badly negative at small r.

The local field factors are plotted in Fig. 3 as a function of wire separation d for carrier density $r_s^e=2$. The local field for the electron wire $G_{ee}(q)$ is sensitive to d for $q/k_F>2$ while the local field for the hole wire $G_{hh}(q)$ is almost independent of d. For $q/k_F \gtrsim 3$ $G_{eh}(q)$ is negative. This reflects the buildup of hole density opposite an electron. For $q/k_F<3$ $G_{eh}(q)$ is positive and this causes the correlation function $g_{eh}(r)$ to drop below unity at intermediate r [see Fig. 1(c)].

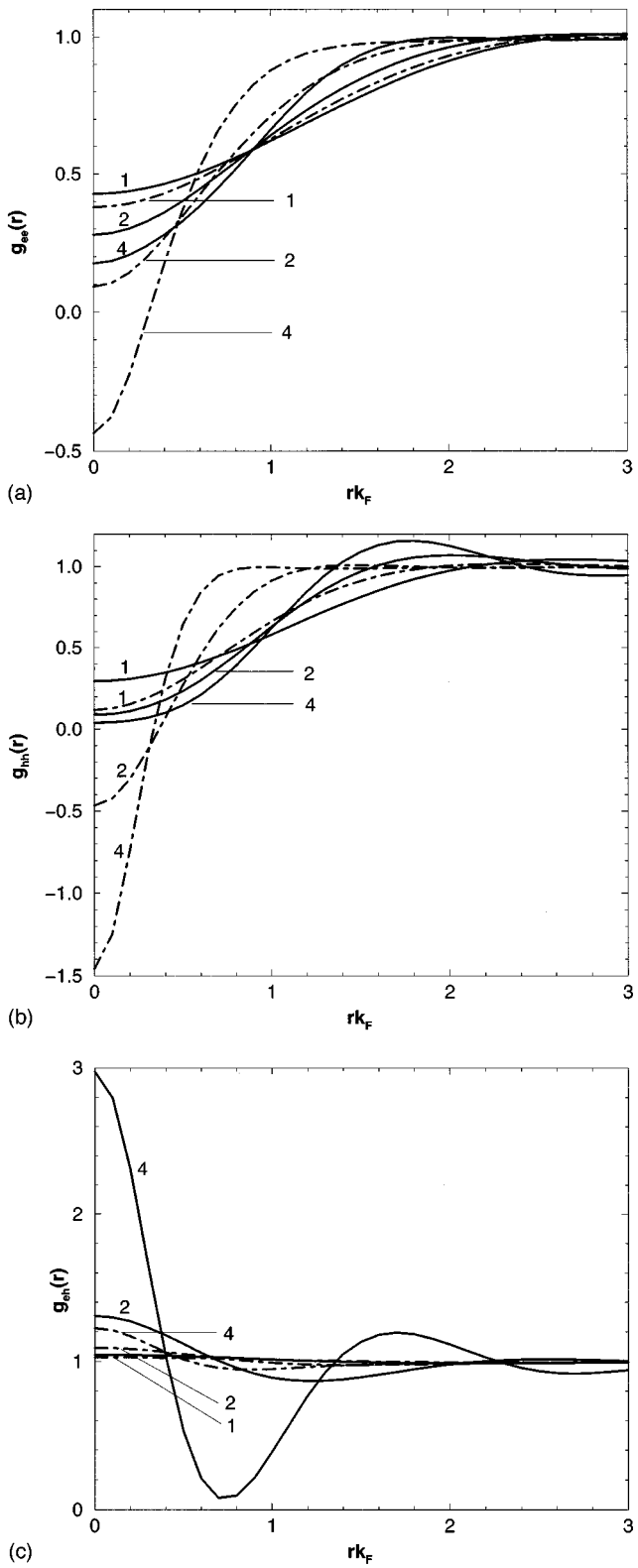

FIG. 2. (a) Pair correlation function for electron wire $g_{ee}(r)$ for wire separation $d/a_0^\star=3.1$. Labels denote electron density parameter r_s^e. Solid lines: present calculation. Dash-dotted lines: RPA. (b) $g_{hh}(r)$ for the same parameters and labels as in (a). (c) $g_{eh}(r)$ for the same parameters and labels as in (a).

$G_{ij}(q)$ goes to zero at small q with a very steep gradient, vanishing only as $\ln q$ [see Eq. (4)]. The reason is associated

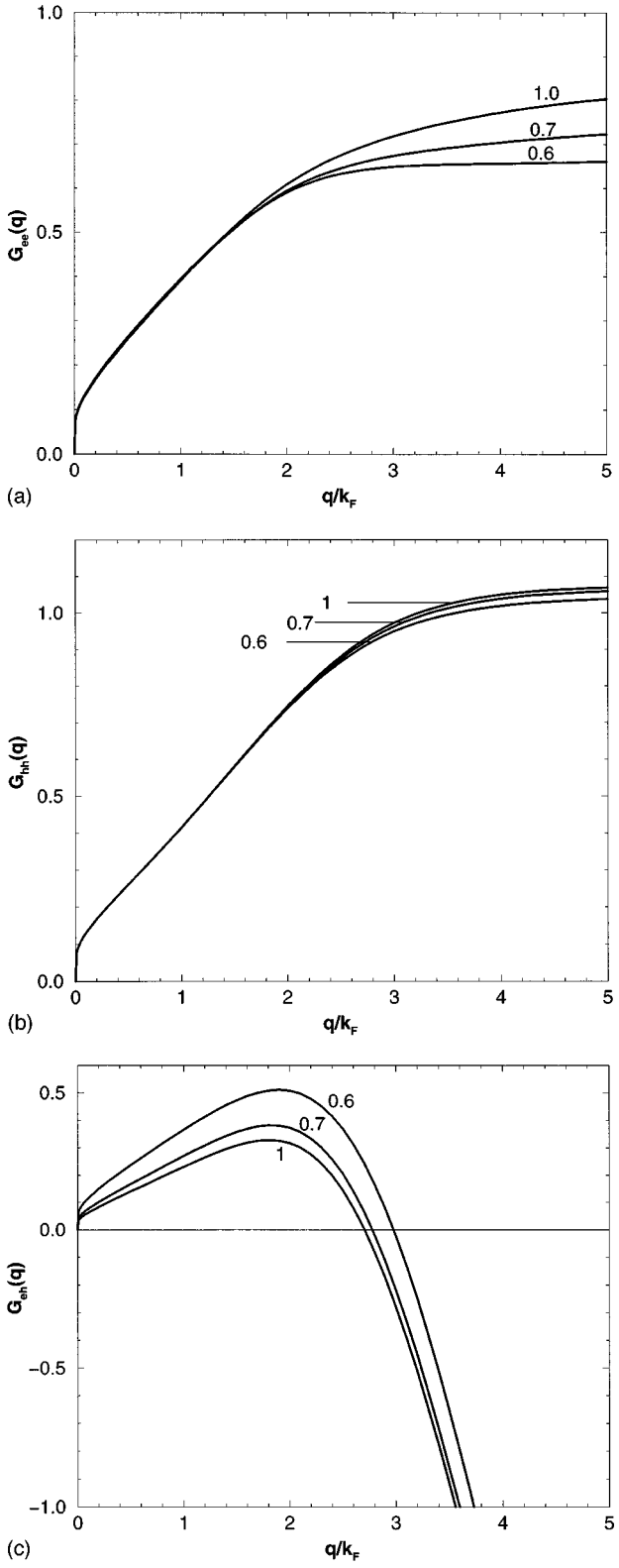

FIG. 3. (a) Local field for electron wire $G_{ee}(q)$. Electron density is $r_s^e=2$. Labels denote wire separation dk_F. (b) $G_{hh}(q)$ for the same parameters and labels as in (a). (c) $G_{eh}(q)$ for the same parameters and labels as in (a).

with the weakly singular nature in one dimension of the Coulomb potential at small q. This behavior is in contrast with two and three dimensions where $G(q)$ vanishes as q and q^2, respectively.

B. Plasmons

The collective modes in single quantum wires have been studied experimentally using spectroscopic methods by Goni *et al.* and Hansen *et al.*[17,18] The carrier densities in the samples studied were relatively high so that correlations would not be expected to be important.

For electron-hole coupled wires the two collective modes are the *acoustic* mode, where the density oscillations in the two wires are in-phase, and the *optic* mode in which the oscillations have opposite phases. The in-phase mode is the more energetic. The collective mode properties are determined by the denominator of the diagonalized matrix elements $\chi_{\pm}(q,\omega)$ [Eq. (6)],

$$D(q,\omega)=[1-\tilde{V}_{ee}(q)\chi_e^{(0)}(q,\omega)][1-\tilde{V}_{hh}(q)\chi_h^{(0)}(q,\omega)] - \tilde{V}_{eh}^2(q)\chi_e^{(0)}(q,\omega)\chi_h^{(0)}(q,\omega). \quad (7)$$

The zeros of the real part of $D(q,\omega)$ give the dispersion of the modes. Their damping is related to the imaginary part of $D(q,\omega)$ by[19]

$$\Delta\omega(q)=\frac{\mathrm{Im}\ D(q,\omega)}{(\partial/\partial\omega)\mathrm{Re}\ D(q,\omega)}. \quad (8)$$

In the small-q limit the solutions are

$$\omega_0^2=\frac{32q^2r_s^e\ln qa}{\pi^2}\Bigg\{1-G_{ee}(q)+\delta_m[1-G_{hh}(q)] \pm\Bigg[\{1-G_{ee}(q)-\delta_m[1-G_{ee}(q)]\}^2 +\left(\frac{2\ln q\sqrt{a^2+d^2}}{\ln qa}\right)^2\delta_m[1-G_{eh}(q)]^2\Bigg]^{1/2}\Bigg\}, \quad (9)$$

where $\delta_m=m_e^\star/m_h^\star$ and the $\pm$ sign corresponds to the optic and acoustic branch, respectively. Equation (9) reduces to

$$\omega_{\mathrm{opt}}=\frac{8q\sqrt{r_s^e\ln qa}}{\pi}\{1-G_{ee}(q)+\delta_m\Delta(d)\}^{1/2},$$

$$\omega_{\mathrm{acou}}=\delta_m\frac{8q\sqrt{r_s^e\ln qa}}{\pi}\{1-G_{hh}(q)-\Delta(d)\}^{1/2}, \quad (10)$$

$$\Delta(d)=\left[\frac{\ln q\sqrt{a^2+d^2}}{\ln qa}\right]^2\frac{[1-G_{eh}(q)]^2}{1-G_{ee}(q)-\delta_m[1-G_{hh}(q)]}.$$

The optic mode depends strongly on the correlations within the electron wire but not the hole wire and is insensitive to the wire separation d. The small-q gradient of the optic mode dispersion curve diverges and always exceeds the initial gradient of the upper boundary of the single-electron excitation region which is $2k_F$. Thus the optic mode always lies above the single-electron excitation region in energy.

The acoustic mode depends on the correlations in the hole wire but not the electron wire, and it is sensitive to d. The small-q gradient of the acoustic mode is finite and the issue of whether its gradient exceeds $2k_F$ or not is determined by d. For large d the acoustic mode at small q lies above the

upper boundary of the single electron excitation region. For small d the mode has crossed over and lies in the undamped region below the lower boundary of the single electron excitation region. In the RPA the wire spacing d for the crossover point where the acoustic plasmon gradient equals the gradient of the upper boundary of the single electron excitation region is given by the analytic expression

$$d = a\left[\exp\left(\frac{\pi^2}{16 r_s^e}\,\frac{1-\delta_m^2}{\delta_m}\right) - 1\right]^{1/2}. \tag{11}$$

This decreases with increasing r_s^e.

In Fig. 4(a) the dispersion of the two collective modes are shown for carrier density $r_s^e = 2$ and wire separation $d = 0.6 k_F^{-1}$. The initial gradient of the optic mode is well separated from the single-electron excitation region. The optic mode in the RPA does not merge with the single-electron excitation region, but approaches it asymptotically in the large-q limit. Correlations reduce the gradient of the curve so that it does intersect with the single-electron excitation region. For larger q the optic mode approaches the collective mode of a single wire of electrons at $r_s^e = 2$. The optic mode is not very sensitive to the wire separation d. For $d \gtrsim 4 k_F^{-1}$ the optic mode is indistinguishable from the single-wire mode.

The energy of the acoustic mode is also suppressed by correlations. The acoustic mode in Fig. 4(a) starts in the undamped finite-q region below the lower boundary of the single-electron excitations and merges with this boundary at $q/k_F \simeq 1.3$. In the single-electron excitation region the acoustic plasmon width $\Delta\omega$ is much smaller than its frequency so the mode is a narrow resonance. This point is discussed below. For $q/k_F = 2.5$ the acoustic mode resonance merges with the curve for a single isolated wire of $r_s^h = 14$ holes. This occurs while it is still inside the single-electron excitation region. As was the case with the optic mode, for $d \gtrsim 4 k_F^{-1}$ the acoustic mode is indistinguishable from the single wire mode for all $q > 0$. The acoustic mode remains well separated from the RPA acoustic mode at small q. This is because in the limit as q approaches zero $G(q)$ goes to zero with a steep gradient. Thus in one dimension the effects of correlations on the plasmon dispersion remain significant even at small but finite q.

We compared the spectral strengths of the collective modes and the single-particle excitations. In the RPA for small q the collective modes saturate the spectral strength. However, we find that correlations reduce the spectral strength of the plasmons and that the contribution to the spectral strength from single-particle excitations takes up the difference. This is similar to the effect we found in a single wire.[13]

Figure 4(b) shows the dispersion of the acoustic mode for $r_s^e = 4$ for a range of wire separations d. For $d \gtrsim k_F^{-1}$ the initial gradient of the acoustic mode curve is greater than $2k_F$ and it lies above the single-electron excitation region. For $d < k_F^{-1}$ it starts in the undamped finite-q region below the single-electron excitations. At all wire separations, for $1 \lesssim q/k_F \lesssim 2$ the modes are almost dispersionless, particularly for larger d. For $q/k_F > 2.6$ the acoustic mode resonance reemerges into the undamped region on the high-q side of the single-electron excitation region. Around $q/k_F = 4$ it becomes degenerate with the boundary of the

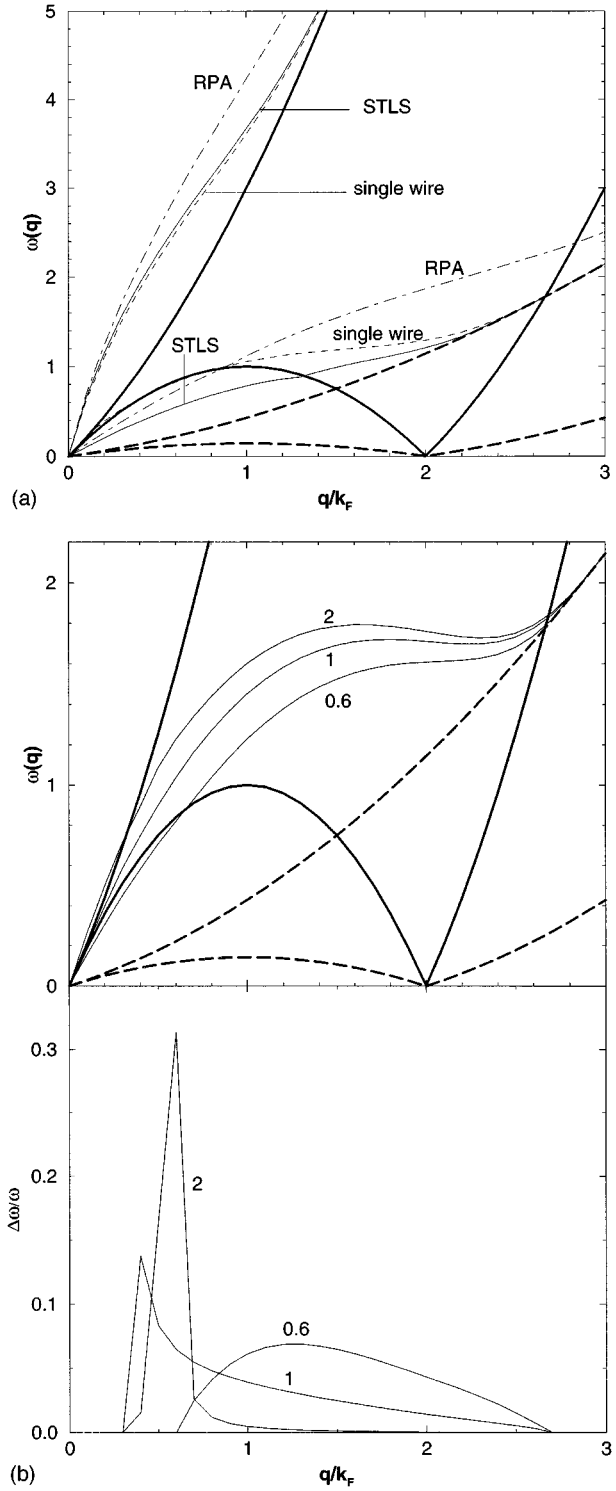

FIG. 4. (a) Optic and acoustic collective mode dispersion curves (thin lines) for $r_s^e = 2$ and wire separation $d = 0.6 k_F^{-1}$. Solid lines: present calculation. Upper dashed line: single-electron wire. Lower dashed line: single-hole wire. Dash-dotted lines: RPA. (The thick solid lines denote the boundaries of the single-electron excitation region; the thick dashed lines are the boundaries for the hole excitations.) (b) Acoustic mode for $r_s^e = 4$. Labels denote wire separation dk_F. Upper panel: dispersion curves. Lower panel: Resonance widths $\Delta\omega/\omega$ inside the single-electron excitation region.

single-hole excitation region, and for $q/k_F > 4$ the damping is very strong and the mode ceases to exist.

Figure 4(b) also shows the relative widths $\Delta\omega/\omega$ of the acoustic modes. In the regions outside the single-electron excitations the modes are undamped. Inside the single-electron excitation region the width of the acoustic mode resonance is narrow, that is, $\Delta\omega/\omega \ll 1$. This is because the acoustic mode at finite q primarily involves density oscillations in the hole wire.[20]

C. Two-body effective interaction

In this section we investigate the possibility that, because the electrons and holes have different effective masses, the retarded screening by the holes of the electron-electron interaction can lead to an attractive effective interaction between the electrons[21] analogous to the Frölich interaction in metals.

We want to construct an effective interaction between two electrons within a medium that includes the holes in the adjacent wire. For a two-component medium of electrons and holes the effective interaction between a test electron embedded in the medium and another electron is given by

$$V_{\rm diel}(q,\omega) = \frac{V_{ee}(q)}{\epsilon(q,\omega)} = V_{ee}(q) + \sum_{i,j=e,h} V_{ei}(q)\chi_{ij}(q,\omega)V_{je}(q). \tag{12}$$

However Eq. (12) does not take into account exchange or correlation effects between the test electron and the medium. To do this we define the dynamic effective interaction as[22]

$$V_{\rm eff}(q,\omega) = V_{ee}(q) + \sum_{i,j=e,h} \tilde{V}_{ei}(q)\chi_{ij}(q,\omega)\tilde{V}_{je}(q) = U_{ee}(q,\omega) + U_{ehe}(q,\omega), \tag{13}$$

where

$$U_{ee}(q,\omega) = V_{ee}(q) + \tilde{V}_{ee}^2(q)\frac{\chi_e^{(0)}(q,\omega)}{1-\tilde{V}_{ee}(q)\chi_e^{(0)}(q,\omega)}, \tag{14}$$

$$U_{ehe}(q,\omega) = \left[\frac{\tilde{V}_{eh}(q)}{1-\tilde{V}_{ee}(q)\chi_e^{(0)}(q,\omega)}\right]^2 \chi_{hh}(q,\omega).$$

In the RPA the $\tilde{V}_{ij}(q)$ are replaced by the bare Coulomb interactions $V_{ij}(q)$ so that $V_{\rm eff}(q,\omega) \equiv V_{\rm diel}(q,\omega)$.

On the other hand, when correlations are strong $V_{\rm eff}(q,\omega)$ and $V_{\rm diel}(q,\omega)$ are quite different, as is shown in Fig. 5(a). The effective interactions are insensitive to ω for small ω so we have set $\omega = 0$. $V_{\rm diel}(q,\omega)$ is strongly attractive for $q/k_F \lesssim 3$ while $V_{\rm eff}(q,\omega)$ is repulsive at small q. In Fig. 5(a) $V_{\rm eff}(q,\omega)$ goes negative when $q/k_F \gtrsim 3$. The RPA interaction between electrons is repulsive for all q. For $q/k_F \lesssim 3$ it is smaller than $V_{\rm eff}(q,\omega)$.

Figure 5(b) shows the dependence of $V_{\rm eff}(q,\omega)$ on the separation between the wires d. Because of the buildup in the electron-hole correlations when the two wires approach each other, the magnitude of the electron-electron interaction mediated by the holes, $U_{ehe}(q,\omega)$, increases rapidly with decreasing d. There is a particularly strong buildup of $U_{ehe}(q,\omega)$ around $q/k_F \simeq 3$. This makes $V_{\rm eff}(q,\omega)$ strongly dependent on d and for sufficiently small d we see that $V_{\rm eff}(q,\omega)$ is attractive for $q/k_F \gtrsim 3.5$. The structure of Eq. (13) is similar to the effective electron-phonon interaction in a conventional BCS superconductor, and the attractive effective interaction raises the interesting possibility of superconducting pairing. This is discussed elsewhere.[23]

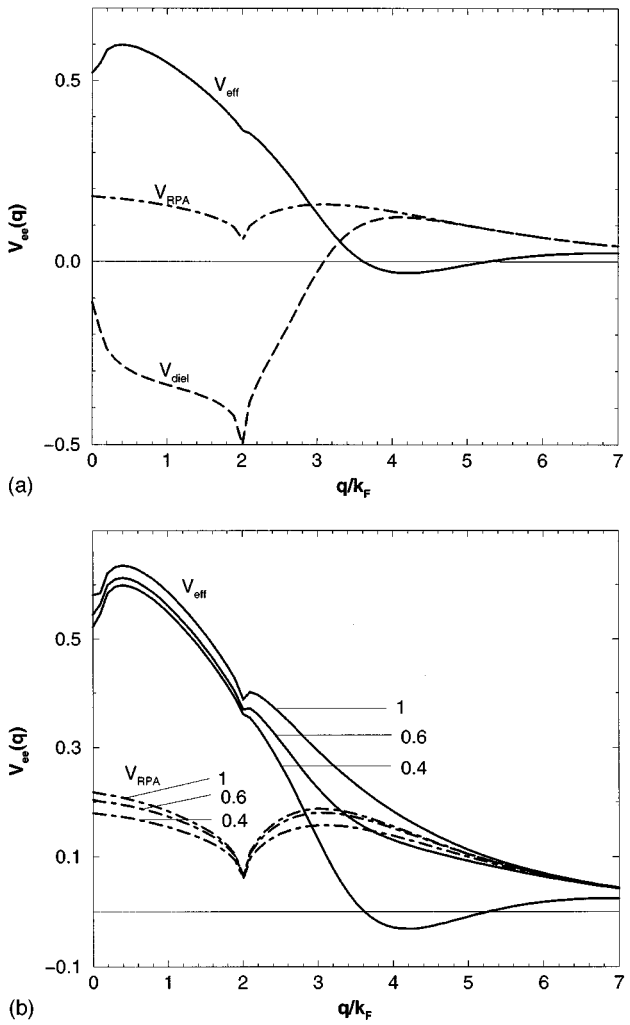

FIG. 5. (a) Comparison of the effective electron-electron interaction mediated by the holes $V_{\rm eff}(q,\omega=0)$ (solid line) obtained from Eq. (13), and $V_{\rm diel}(q,\omega=0)$ (dashed line) obtained from Eq. (12). Also shown is the electron-electron interaction within the RPA (dash-dotted line). Electron density parameter is $r_s^e = 2.5$. Wire separation is $dk_F = 0.4$. (b) Dependence of the effective electron-electron interaction mediated by the holes $V_{\rm eff}(q,\omega=0)$ (solid lines) on the wire separation dk_F as labeled. Dash-dotted line is the RPA result.

In contrast to $V_{\rm eff}(q,\omega)$, the $V_{\rm diel}(q,\omega)$ is attractive for $q/k_F \lesssim 3$ for all values of d. This is due to the fact that without the correlations between the test electron and the medium, the attractive interaction between the test electron and the medium dominates over the direct interaction of the test electron with the other electron.

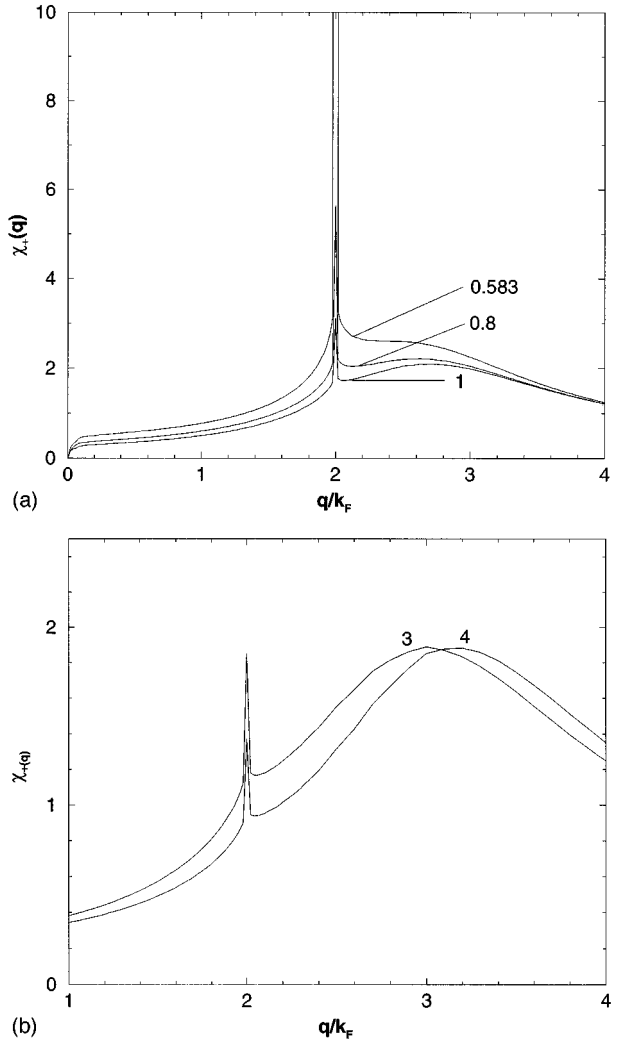

FIG. 6. (a) Static response function $\chi_+(q)$ at $r_s^e=2$ for wire separations dk_F as labeled. As dk_F approaches 0.583 $\chi_+(q)$ diverges at $q/k_F=2$. (b) $\chi_+(q)$ at $r_s^e=3$ and $r_s^e=4$ as labeled. The wire separation is $d/a_0^\star=2.8$. There is no divergence. Note the peak around $q/k_F=3$.

IV. CHARGE-DENSITY WAVES

The possibility of a charge-density-wave instability in a single quantum wire was investigated by Das Sarma and Lai,[24] who found a strong peak in $\chi(q)$ at $q=2k_F$ for temperatures $kT<0.1E_F$ and collisional broadening $\gamma<0.1E_F$, where E_F is the Fermi energy. The charge-density-wave instability for two coupled electron wires was investigated by Gold[1] using the Hubbard approximation for the local field. Gold identified a charge-density-wave instability in the long-wavelength limit. The charge-density-wave instability in a double quantum wire was recently calculated by Wang and Ruden[25] using a STLS local field for correlations within each wire but neglecting the correlations between the wires. Without the electron-hole correlations the wire spacing at which the instability occurs will be overestimated. Basing their argument on a total energy calculation in Ref. 3 Wang and Ruden found when the wire separation is small that there is a charge-density-wave instability at low carrier densities.

In our approach we include the STLS local fields not only within each wire but also between the wires. We search for a divergence in $\chi_+(q)=\chi_+(q,\omega=0)$ [see Eq. (6)]. Figure 6(a) shows the static response function $\chi_+(q)$ at $r_s^e=2$ for a range of wire separations d. When d approaches $0.583k_F^{-1}$ there is a divergence in $\chi_+(q)$ at $q/k_F=2$. The divergence indicates that the electron and hole liquids are unstable to infinitesimal periodic perturbations of the density with wave number $q/k_F=2$, that is to a charge-density-wave ground state. For $0.8<r_s^e<2.5$ the divergence in $\chi_+(q)$ remains at $q/k_F=2$.

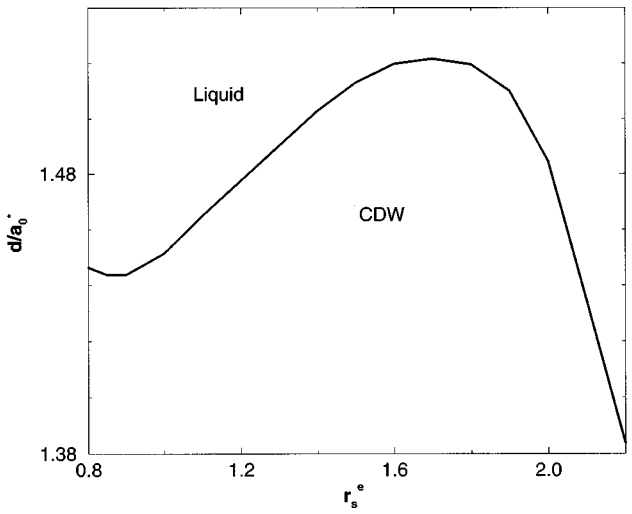

FIG. 7. Phase boundary for charge-density-wave ground state for wire separation dk_F and carrier density r_s^e.

For $q/k_F=2$ the free-particle static susceptibility $\chi^{(0)}(q)$ diverges[26] so that $\chi_\pm(q)$ is independent of $\chi^{(0)}(q)$. In this case the condition for $\chi_+(q)$ to diverge at $2k_F$ reduces to

$$\left[\frac{V_{ee}(q)}{V_{eh}(q)}\right]^2=\frac{[1-G_{eh}(q)]^2}{[1-G_{ee}(q)][1-G_{hh}(q)]},\quad q=2k_F. \tag{15}$$

For $r_s^e>2.5$ the peak in $\chi_+(q)$ does not diverge even when d is small. Figure 6(b) shows that as r_s^e increases there is a peak that moves away from $q/k_F=2$ and towards $q/k_F=4$. This effect may be a precursor to the formation of a Wigner crystal.[27]

In the RPA the right-hand side of Eq. (15) is unity and there will always be an instability when $d=0$. Thus in the RPA the coupled electron-hole wire always has a $2k_F$ charge-density-wave instability when the two wires are overlapping.

The transition to the charge-density-wave ground state is controlled by the competition between the correlations within each wire and the correlations between the wires. Figure 7 shows the boundary between the liquid and charge-density-wave ground states as a function of wire separation d and carrier density r_s^e. When d is large the attractive correlations between the wires are too weak for a charge-density-wave state to be stable. For $r_s^e\lesssim 0.8$ the degeneracy energy is too large for the transition to occur at any d. As r_s^e increases above 0.8 it becomes easier to form the charge-density wave and the transition occurs at larger values of d. However, repulsive correlations within the wires increase with r_s^e. For $r_s^e>1.7$ these correlations make it more difficult

to form charge-density waves, which require the carriers to group. Thus for $r_s^e > 1.7$ the transition occurs at decreasing d. When this effect becomes dominant by $r_s^e \geq 2.5$ there is no stable charge-density-wave ground state at any d.

V. CONCLUSIONS

Coupled electron-hole wires differ in several important respects from coupled electron-electron wires. The different effective masses make the system asymmetric. The attractive interaction between the electrons and holes leads to much stronger correlations between the wires and these correlations can in turn affect the correlations between carriers in the same wire. Both the static and dynamic properties of the wire with the smaller r_s are strongly affected by the presence of a second wire, while the larger r_s wire's properties are not sensitive to the second wire.

We find for $r_s^e \geq 2$ that correlations are very important and that RPA breaks down at small r. The correlations depress the energy of the collective modes of the system. The correlations are found to reduce the spectral strength of the collective modes. The single-particle excitations take up the difference by significantly contributing to the total spectral strength.

The asymmetry of the system allows the acoustic plasmon to survive as a sharp resonance peak after it enters the single-electron excitation region. The acoustic plasmon can appear on the undamped high-q side of the single-electron excitation region.

The retarded effective electron-electron interaction can become attractive for intermediate momentum transfers. This effect is possible because of the strong buildup of correlations between the electrons and the heavier holes. It raises the possibility of bound pairs of electrons forming in the electron wire. We also found there is an instability towards a charge density-wave ground state of wave number $q/k_F = 2$ for the range of densities $0.8 \lesssim r_s^e \lesssim 2.5$ when the wires reach a critical separation.

ACKNOWLEDGMENTS

This work was supported by an Australian Research Council Grant. We thank G. La Rocca, M. Tosi, and J. Voit for useful discussions. D.N. thanks F. Bassani for the hospitality and facilities of the Scuola Normale Superiore.

[1] A. Gold, Philos. Mag. Lett. **66**, 163 (1992).
[2] W. Que and G. Kirczenow, Phys. Rev. B **37**, 7153 (1988).
[3] Z. Wu and P.P. Ruden, J. Appl. Phys. **71**, 1318 (1992).
[4] C. Eugster and J.A. del Alamo, Appl. Phys. Lett. **60**, 642 (1992).
[5] Q.P. Li and S. Das Sarma, Phys. Rev. B **43**, 11 768 (1991).
[6] A. Gold and A. Ghazali, Phys. Rev. B **41**, 7626 (1990); A. Gold, Z. Phys. B **89**, 213 (1992).
[7] B.Y.-K. Hu and S. Das Sarma, Phys. Rev. Lett. **68**, 1750 (1992); Phys. Rev. B **48**, 5469 (1993).
[8] K.S. Singwi, M.P. Tosi, R.H. Land, and A. Sjölander, Phys. Rev. **176**, 589 (1968).
[9] A. Sjölander and J. Stott, Phys. Rev. B **5**, 2109 (1972).
[10] W.I. Friesen and B Bergersen, J. Phys. C **13**, 6627 (1980).
[11] A.N. Borges, M.H. Degani, and O. Hipolito, Superlattices Microstruct. **13**, 375 (1993).
[12] V.B. Campos, M.H. Degani, and O. Hipolito, Superlattices Microstruct. **17**, 85 (1995).
[13] J.S. Thakur and D. Neilson, Phys. Rev. B (to be published).
[14] L. Świerkowski, D. Neilson, and J. Szymański, Phys. Rev. Lett. **67**, 240 (1991).
[15] P.F. Williams and A.N. Bloch, Phys. Rev. B **10**, 1097 (1974).
[16] Lerwen Liu, L. Świerkowski, and D. Neilson (unpublished).
[17] A.R. Goni, A. Pinczuk, J.S. Weiner, J.M. Calleja, B.S. Dennis, L.N. Pfeiffer, and K.W. West, Phys. Rev. Lett. **67**, 3298 (1991); A. Schmeller, A.R. Goni, A. Pinczuk, J.S. Reiner, J.M. Calleja, B.S. Dennis, L.N. Pfeiffer, and K.W. West, Phys. Rev. B **49**, 14 778 (1994).
[18] W. Hansen, M. Horst, J.P. Kotthaus, U. Merkt, Ch. Sikorski, and K. Ploog, Phys. Rev. Lett. **58**, 2586 (1987); T. Demel, D. Heitman, P. Grambow, and K. Ploog, Phys. Rev. B **38**, 12 732 (1988).
[19] A.L. Fetter and J.D. Walecka, *Quantum Theory of Many Particle Systems* (McGraw-Hill, New York, 1971), p. 180.
[20] Lerwen Liu, L. Świerkowski, J. Szymański, and D. Neilson, Phys. Rev. B **53**, 7923 (1996).
[21] J.S. Thakur, D. Neilson, and M.P. Das, Bull. Am. Phys. Soc. **40**, F12 (1995); P.M. Platzman and T. Lenosky, Phys. Rev. B **52**, 10 327 (1995).
[22] G. Vignale and K.S. Singwi, Phys. Rev. B **31**, 2729 (1985).
[23] J.S. Thakur and D. Neilson (unpublished).
[24] S. Das Sarma and Wu-yan Lai, Phys. Rev. B **32**, 1401 (1985).
[25] R. Wang and P.P. Ruden, Phys. Rev. B **52**, 7826 (1995).
[26] R.E. Peierls, *Quantum Theory of Solids* (Oxford, Clarendon, 1955).
[27] T. Schulz, Phys. Rev. Lett. **71**, 1864 (1993).